electronics

MDPI

Article

HTC-Grasp: A Hybrid Transformer-CNN Architecture for Robotic Grasp Detection

Qiang Zhang [1], Jianwei Zhu [1], Xueying Sun [1,*] and Mingmin Liu [2]

[1] School of Automation, Jiangsu University of Science and Technology, No. 666 Changhui Road, Zhenjiang 212100, China
[2] Central Research Institute, SIASUN Robot & Automation Co., Ltd., No. 16 Jinhui Street, Shenyang 110168, China
* Correspondence: sunxueying@just.edu.cn

Abstract: Accurately detecting suitable grasp areas for unknown objects through visual information remains a challenging task. Drawing inspiration from the success of the Vision Transformer in vision detection, the hybrid Transformer-CNN architecture for robotic grasp detection, known as HTC-Grasp, is developed to improve the accuracy of grasping unknown objects. The architecture employs an external attention-based hierarchical Transformer as an encoder to effectively capture global context and correlation features across the entire dataset. Furthermore, a channel-wise attention-based CNN decoder is presented to adaptively adjust the weight of the channels in the approach, resulting in more efficient feature aggregation. The proposed method is validated on the Cornell and the Jacquard dataset, achieving an image-wise detection accuracy of 98.3% and 95.8% on each dataset, respectively. Additionally, the object-wise detection accuracy of 96.9% and 92.4% on the same datasets are achieved based on this method. A physical experiment is also performed using the Elite 6Dof robot, with a grasping accuracy rate of 93.3%, demonstrating the proposed method's ability to grasp unknown objects in real scenarios. The results of this study indicate that the proposed method outperforms other state-of-the-art methods.

Keywords: robotic grasp; transformer; attentional mechanism

Citation: Zhang, Q.; Zhu, J.; Sun, X.; Liu, M. HTC-Grasp: A Hybrid Transformer-CNN Architecture for Robotic Grasp Detection. *Electronics* **2023**, *12*, 1505. https://doi.org/10.3390/electronics12061505

Academic Editors: Pei-Chi Huang and Wei Fang

Received: 13 February 2023
Revised: 11 March 2023
Accepted: 20 March 2023
Published: 22 March 2023

1. Introduction

In the most recent decade, the advancement of artificial intelligence has made smart robots increasingly important in industries such as smart factories and healthcare [1,2]. Among the tasks performed by these robots, grasping objects is a fundamental ability that enables them to carry out more complex operations. Vision-based automated grasping, where the robot uses visual sensors to identify the best gripping position for an object, is crucial for their intelligence and automation [3,4]. However, despite the advancements in the field, most of the current methods are still limited to models of known objects or trained for known scenes, making the task of grasping unknown objects, with high accuracy, a significant challenge [5].

Currently, most grasp detection methods for vision robots rely on convolutional neural networks (CNNs) [6–10]. Despite their popularity, CNNs have limitations in handling grasping tasks. They are designed to process local information through their small convolutional kernels and have difficulty capturing global information due to limited filter channels and convolution kernel sizes. The convolutional computation method used by CNNs also makes it challenging to capture long-distance dependency information during information processing.

Transformer architecture has seen great success in the field of vision lately [11,12]. The Transformer's self-attention mechanism provides a more comprehensive understanding of image features compared to CNNs. The Transformer has the ability to effectively

capture global information through its self-attentive mechanism, which makes it a more representative model.

While the self-attention mechanism of the Transformer is useful for capturing information within a single sample, it may not fully leverage the potential connections between different samples. In the task of grasping, the features of the grasping target are often correlated, and the background features of similar scenes are consistent. Thus, considering the potential connections between different samples can lead to a more robust feature representation. To address this challenge, the proposed HTC-Grasp incorporates external attention in the transformer block to enhance the representation of correlations between different images.

Moreover, the multi-scale feature fusion mechanism introduces a significant amount of noisy features, which can negatively impact grasp detection performance. To mitigate this issue and improve the role of effective features, the proposed framework incorporates a residual connection-based channel attention block in the decoder. This approach enables efficient learning of discriminative channel-wise features.

The original contributions of this research are outlined below:

1. A highly robust hierarchical Transformer-CNN architecture for robot grasp detection is developed that integrates local and global features.
2. In this architecture, the external attention-based hierarchical Transformer is proposed as an encoder to effectively capture global context and the correlation features across the whole data. Furthermore, a channel-wise attention-based CNN decoder is provided to adaptively adjust the weight of the channels, thus providing a more efficient feature aggregation.
3. Extensive experiments are conducted on both public datasets and real-world object grasp tasks to validate the performance of the HTC-Grasp approach. The results, both qualitative and quantitative, manifest that the HTC-Grasp surpasses state-of-the-art robotic grasp solutions and can detect stable grasps with high accuracy.

The proposed HTC-Grasp approach can adapt well to the 2D robotic grasp environment and can be applied in logistics centers for picking up goods, automated garbage sorting, robotic assistance for household tasks, etc.

2. Related Works

The representation of object grasping is crucial for robot grasp detection. Jiang et al. [13] proposed an efficient method that describes the grasping position using a rectangular representation, using a 5-dimensional vector to describe the position, height, width, and rotation angle of the grasp in the image. Morrison et al. [14] introduced a grasp location description method, which gives the gripping position and posture by predicting the gripping quality of each pixel. These two models are widely used in robot grasp detection tasks.

Current grasp detection models are broadly classified into two different types: cascade approaches and one-stage architecture. Cascade approaches perform the entire grasp prediction process in stages, including the extraction of target features, generation of candidate regions, and evaluation of the optimal gripping position. Lenz et al. [15] created the Cornell dataset and proposed a two-stage cascade detection model to learn this five-dimensional grasp. The first stage uses a neural network to extract grasp prediction features. The second phase refines the predicted grasp parameters to output the optimal grasp location. Zhou et al. [16] presented a model that predicts multiple grasping poses using an oriented anchor box. Zhang et al. [3] introduced the ROI-GD approach, which uses ROI features to detect grasps instead of the whole image. Laili et al. [17] presented a region-based approach to locating grasping point pairs. A consistency-based method is used to train the grasp detector with less labelled training data.

In the last few years, the development of one-stage detection approaches for object grasping has gained popularity due to their simple and efficient structure. The one-stage approach trains a grasp detection model to directly output the grabbing location. Previous works, such as Redmon et al. [18], used AlexNet to directly process the input image and

predict the grasp location. Kumra et al. [19,20] built a grasp network based on ResNet that extracts features from RGB and depth images to output both classification and regression results for the optimal grasp location. Mahler et al. [21] put forward a grasp quality evaluation network using image segmentation and a corresponding point cloud for grasp prediction. Morrison et al. [14] used convolutional layers for encoding and decoding to perform pixel-level grasp prediction of feature maps. Yu et al. [22] presented a U-Net-like architecture with channel attention modules to better utilize features. Wu et al. [23] introduced an anchor-free approach which employs a completely convolutional network. This approach frames grasp detection as grasp rectangle regression and category classification tasks. The CNN-based grasping target detection algorithms discussed above have made significant progress. However, the use of convolutional kernels, which primarily focus on local spatial information, can limit the ability to capture global information correlations, potentially hindering further improvements in detection accuracy.

Recently, the transformer has gained traction in computer vision because of its ability to capture global information, overcoming the limitations of CNN models. The transformer has shown excellent performance in applications like object detection, classification and tracking [24,25] through its self-attention mechanism and pyramid-like structure. In 2022, Wang et al. [26] used the SWIN Transformer to extract features with impressive results. The self-attentive mechanism, while useful, has a limitation in that it focuses only on the information contained within a single sample and ignores the connection across the whole dataset, which may negatively impact the robustness of feature representation.

To overcome the challenges described above, the HTC-Grasp approach is proposed in this article. With the aid of external attention structure, long-distance spatial correlation can be learned. The global context between data samples can ameliorate feature robustness implicitly. In order to aggregate the extracted multiscale features, up-sampling and skip connection are introduced to the decoder. The channel attention modules based on SE-block further assign adaptive weights to each feature channel to enhance the feature representation.

3. Method

3.1. Grasp Task Representation

The vision grasping tasks typically involve collecting visual images of the target object using sensors such as RGBD cameras. These images are processed by a model to determine the optimal grasp position. When the robot is equipped with parallel grippers, the grasping parameters p can be represented as a 5-dimensional tuple.

$$p = \{x, y, \theta, w, h\} \tag{1}$$

When it comes to the above formula, (x, y) means the 2D coordinates of the center point, (w, h) represents the size of the grasping box including the width and height. What's more, θ represents the rotation angle of the gripper compared to the horizontal axis.

An alternative representation for high-precision, real-time robot grasping was introduced in [14]. In this representation, the grasp is redefined for 2DoF robotic grasping tasks as follows:

$$P = \{Q_g, \Theta_g, W_g\} \in \mathbb{R}^{3 \times W \times H} \tag{2}$$

where P is a 3-dimensional tensor. The first dimension, Q_g means the quality of every pixel of the input image. And the second dimension, Θ_g, denotes the orientation angle between the fingertips of the gripper. What's more, the third dimension, W_g, represents the opening width between the fingertips of the gripper. Each pixel, with a specific angle $\Theta_{g_{i,j}}$ and width $W_{g_{i,j}}$, corresponds to the orientation angle and width of the finger gripper at the particular position. Additionally, H and W correspond to the width and length of the feature map.

3.2. Grasp Overview

The structure of the HTC-Grasp is illustrated in Figure 1. It consists of three parts: the Transformer based encoder, the CNN-based decoder, and the prediction head. The

encoder is built using hierarchical transformers with a pyramidal design to extract multi-scale features. The CNN-based decoder, made up of transposed convolution layers with res-channel attention blocks, fuses the previously obtained multi-scale features. Finally, the fused features are used by four sub-task networks to predict grasp heatmaps, including the map of quality score, the angle (in $\sin 2\theta$ and $\cos 2\theta$ form) and the width.

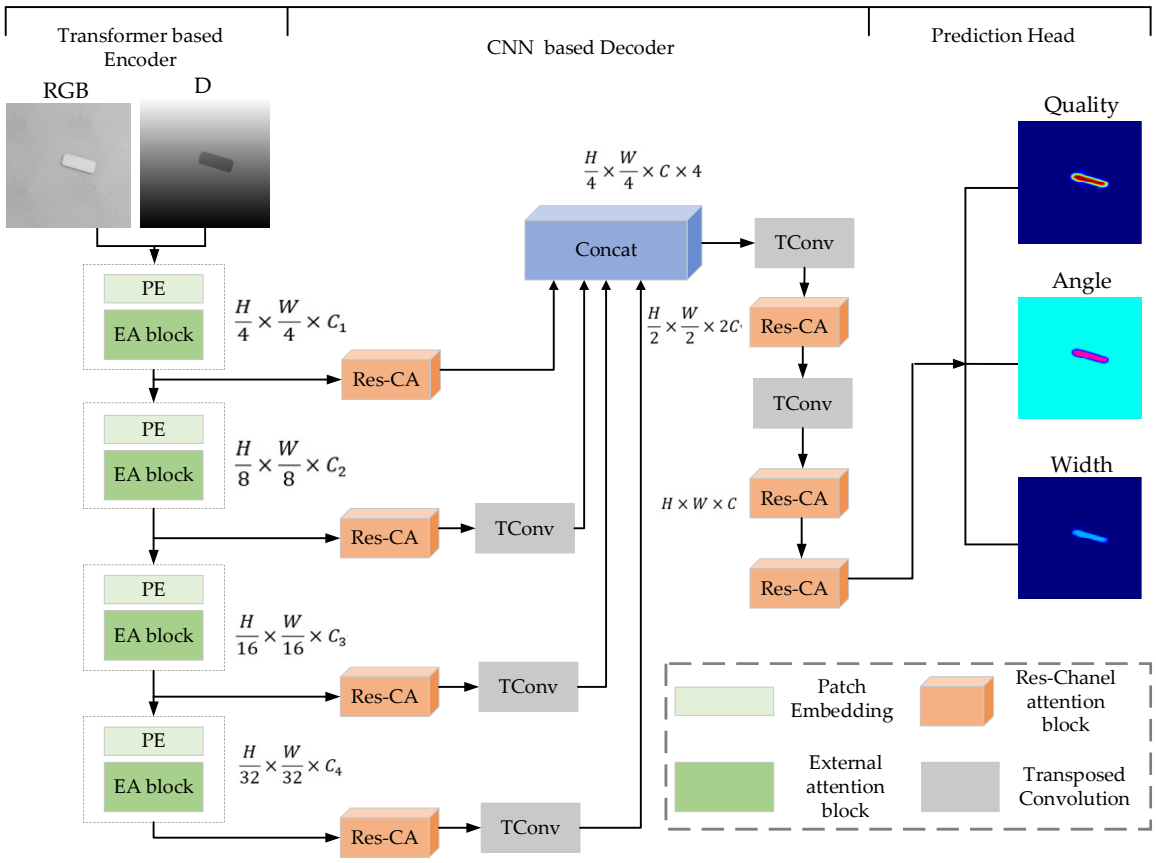

Figure 1. Overview of HTC-Grasp. H and W in the figure correspond to the height and width of the feature map. C_i is the channel size of the feature map.

The specific process is as follows. Inputting an RGB-D image with the size $H \times W \times 4$, it is first divided into blocks with 4×4 pixels for each block. These blocks are then used as inputs to the transformer blocks, which output multi-level feature images with resolutions of $\{1/4, 1/8, 1/16, 1/32\}$ of the original image. These multi-level features are then up-sampled to $56 \times 56 \times C_i$ based on the transparent convolutional layers. By employing channel-wise concatenation, the four levels of features are aggregated. To make the height and width of the obtained features consistent with the original data, the two deconvolution modules further up-sample the features. Two Res-channel attention blocks are also employed to enhance the robustness of the features in the last part of the decoder. The prediction head then can predict quality, angle and width heatmaps. The details of HTC-Grasp are explored in the subsequent sections.

3.3. HTC-Grasp Architecture

3.3.1. Hierarchical Transformer Encoder

To facilitate the generation of multi-scale feature maps, HTC-grasp exploits a layered Transformer architecture in this article. Multi-scale features generated by the hierarchical Transformer encoder enhance the capability of the model. The feature encoder of HTC-Grasp comprises four stages, each designed to generate feature maps at a different scale.

The structure of each stage is similar and consists of a transformer block and a patch embedding layer.

To be more specific, an image with resolution $H \times W \times 4$ is fed into Patch Embedding stages to get a hierarchical feature image F_i with the resolution of $\frac{H}{2^{i+1}}, \frac{W}{2^{i+1}}, C_i$, where i ranges from 1 to 4. Considering that uniform partitioning will make the obtained patches have no overlapping parts and weaken the connection between patches, overlapping parts between each patch in the partitioning are preserved intentionally. Then the image patches are fed into the encoder to obtain multi-scale features.

The Transformer based encoder is designed to extract features. Self-attention is the most important module of each Transformer block. The original self-attention mechanism generates three matrices: the query matrix $Q \in \mathbb{R}^{N \times d_k}$, the key matrix $K \in \mathbb{R}^{N \times d_k}$, and the value matrix $V \in \mathbb{R}^{N \times d_v}$. Here, N means the number of patches. d_k signifies the feature dimensions of Q and K. d_v corresponds to the dimension of V. The calculation of self-attention is as follows:

$$Attention = softmax\left(\frac{QK^T}{\sqrt{d}}\right)V \tag{3}$$

The shortage of self-attention presents a significant drawback to real-time applications, especially extremely complex calculations. Additionally, self-attention can only model correlations within individual samples, ignoring the correlations across the entire dataset. To overcome these limitations, HTC-Grasp redesigns the Transformer blocks through the multi-head external attention (MEA) [27] blocks.

MEA mechanism is incorporated to improve the efficiency of the transformer layer. This mechanism is represented by the following equations:

$$h_i = ExternalAttention(F_i, M_k, M_v) \tag{4}$$

$$F_{out} = MultiHead(F, M_k, M_v) \tag{5}$$

$$F_{out} = Concat(h_1, \ldots, h_H)W_o \tag{6}$$

where h_i stands for the ith multi-head, H symbolizes the total number of multi-heads, and W_o is a linear transformation matrix that has equal output and input dimensions. The structure of MEA is shown in Figure 2.

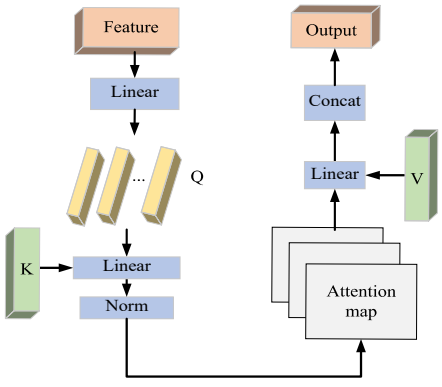

Figure 2. The architecture of external attention block.

3.3.2. Grasp Decoder

The grasp decoder is designed with a combination of convolutional layers and Res-channel attention blocks. As can be seen in Figure 3, the Res-channel attention block is a combination of a ResNet block and a channel attention block. The ResNet block is made up of three convolutional blocks. The kernel sizes of these three convolutional blocks are set o 1×1, 3×3 and 1×1, respectively. The channel attention block, on the other hand,

utilizes global average pooling (GAP) aiming at decreasing the number of participants contained in the features. This block then consists of dual fully connected layers and one ReLU unit, which utilizes global information to selectively emphasize important features and reduce the emphasis on less relevant features.

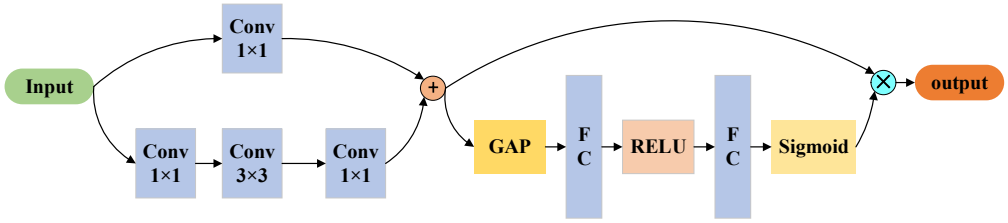

Figure 3. Res-Channel attention block.

Specifically, the decoder involves three key steps. To begin with, the multilevel features F_i from the encoder are fed through the up-sample block, which increases the resolution to $1/4 \times 224 \times 224$, and then these features are concatenated. Next, a CNN layer is utilized to merge the resulting features, and this is followed by two upsampling layers that increase the resolution to 224×224. Finally, the fused features are utilized to make predictions regarding the grasp heatmaps.

3.3.3. Loss Function

In this study, the task of robot grasp detection is a one-stage structure. In addition, the smooth L_1loss function is adopted as the optimization objective. The advantage of this loss function is that it is robust to outliers and can provide stability during training.

$$L_{reg}(\hat{T}_k, T_k) = \sum_{k \in \{q, \sin 2\theta, \cos 2\theta, w\}} Smooth(\hat{T}_k - T_k) \tag{7}$$

The Smooth L_1loss is defined as follows:

$$Smooth_{L1}(x) = \begin{cases} 0.5x^2, & if|x| < 1 \\ |x| - 0.5, & otherwise \end{cases} \tag{8}$$

In this work, $\hat{T}_k$ means the predicted grasping parameters. T_k represents the ground truth. What's more, q represents the grasping quality, θ stands for the rotation angle, and w means the opening width between the fingertips of the gripper.

4. Experiments and Results

4.1. Dataset

In this work, experiments are conducted on Cornell and Jacquard datasets to fully validate our HTC-Grasp method.

(a) Datasets

The Cornell dataset was published in 2013 and it includes 240 distinct objects. It consists of 885 color images and 885 depth images. To ensure the best results from the transformer structure, which requires a substantial amount of data, data augmentation approaches like image rotation, scaling, and random cropping are applied to the dataset in our work.

The Jacquard dataset consists of 54,485 diverse scenes for 11,619 different objects. It provides RGB images, 3D point cloud data, and grasp annotations for each scene. Given the massive size of the Jacquard dataset, no data transformations are performed on it in this work.

(b) Implementation details

In this article, the model was constructed using the Pytorch framework on the Ub-untu 20.04 platform. For training, an NVIDIA RTX 3090Ti GPU and an Intel Core i9-12900K CPU are utilized. In the data augmentation process for the Cornell dataset, each 640 × 480 image undergoes rotation, scaling, and random cropping, resulting in an image of size 224 × 224. During each training step, image samples were randomly selected from the training dataset, with 200 batches of size 32 in each epoch, and 100 epochs are trained in total. AdamW is employed for training HTC-Grasp architecture. The starting learning rate is preset to 0.0001.

HTC-Grasp is parameterized with the following configuration. The channel numbers for stages 1 to 4 are set to 2^5, 2^6, 2^7 and 2^8 respectively. The headcount for each external attention layer is set to 1, 2, 4, and 8, respectively. The number of encoder layers in stages 1 to 4 is set to $L_1 = L_2 = L_3 = L_4 = 2^8$. The number of output feature channels for each decoder is set to $C = 2^8$.

In this work, each dataset was structured in two portions, with 90% used for training and 10% for testing. To measure the capabilities of the HTC-Grasp method, both image-wise and object-wise detection accuracy was used. Image-wise split randomly assigns the entire data set as 9:1 to assess HTC-Grasp's generalization performance of previously seen objects when they appear in different situations and orientations. Object-wise split divides the dataset based on object instances, ensuring that there are no identical object instances in the training and test sets, thereby testing the network's ability to generalize to unknown objects.

(c) Evaluation index

The predicted grasping box was considered correct if it meets the following angle and IOU constraints.

(1) The angle error between the predicted and labeled values must be within $\pi/6$
(2) The IOU index, which is defined in Equation (9), must be greater than 0.25.

$$IOU(R^*, R) = \frac{|R^* \cap R|}{|R^* \cup R|} \tag{9}$$

4.2. Comparison Studies

To compare HTC-Grasp and other recent grasp detection methods, the same evaluation metrics were used.

The comparison study starts with the evaluation of the Cornell dataset. The grasp position can be determined by the four heatmaps output. The center pixel at the most likely grasp position has the maximum predicted value of quality. The size and rotation values of the grasp rectangle can be obtained by indexing the other three parameter values corresponding to the center pixel. Figure 4 presents the results of GR-CNN, TF-Grasp [26] and the proposed HTC-Grasp for unseen objects on the Cornell dataset. Statistical results in Table 1 indicate that HTC-Grasp has a higher grasp quality as compared to the GR-CNN and TF-Grasp methods.

For the classical method experimental results presented in Table 1, the data reported in their original paper are selected. Table 1 illustrates the performance of HTC-Grasp compared to existing algorithms on the Cornell dataset. HTC-Grasp surpasses other algorithms with accuracy rates of 98.3% and 96.9% on image and object-wise tests, respectively. Furthermore, HTC-Grasp, utilizing the NVIDIA RTX 3090Ti GPU, processes a single frame in approximately 5.4 ms, fulfilling the requirement for real-time processing.

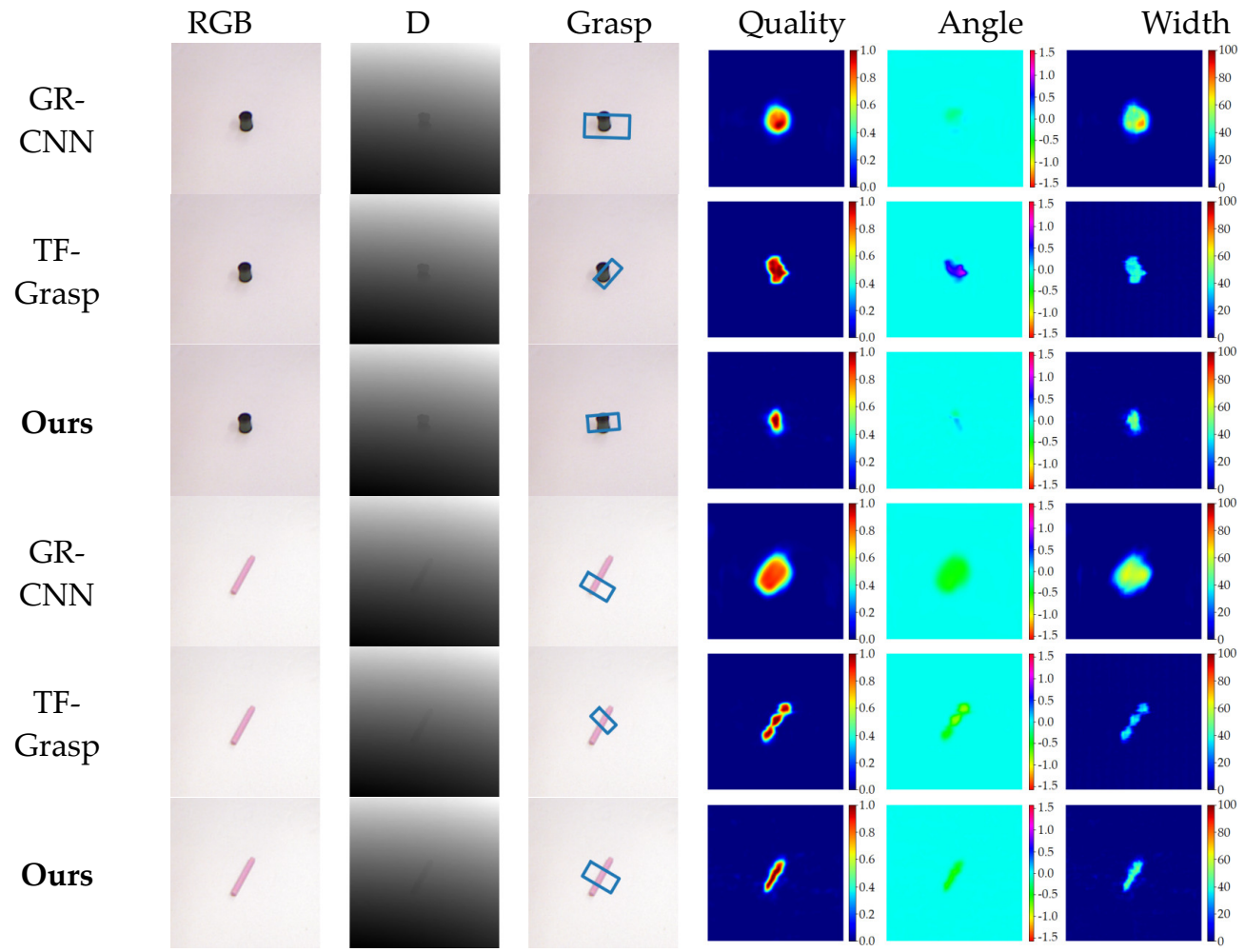

Figure 4. Comparison of predicted heatmaps on Cornell Dataset. The first and second columns depict RGB and depth images, respectively. The third column displays the grasping rectangles and successful grasps are marked as rectangles. The final three columns depict heatmaps indicating the quality, angle, and width of the detected grasps. The quality heatmaps characterizes the degree of confidence that each pixel is a valid grasping location.

Table 1. The statistical results on Cornell Dataset.

Researchers	Approaches	Data	Accuracy (%)		Time (ms)
			Image-Wise	Object-Wise	
Lenz [15]	SAE	RGB-D	73.9	75.6	1350
Redmon [18]	AlexNet	RGB-D	88	87.1	76
Kumra [19]	ResNet-50 × 2	RGB-D	89.2	88.9	103
Morrision [14]	GG-CNN	D	73	69	19
Chu [28]	ResNet-50	RGB-D	96	96.1	120
Asif [8]	GraspNet	RGB-D	90.2	90.6	24
Kumra [20]	GR-CNN	RGB-D	97.7	96.6	20
Wang [26]	TF-Grasp	RGB-D	97.99	96.7	41.6
Ours	HTC-Grasp	RGB-D	**98.3**	**96.9**	**5.4**

Comparative experiments using the Jacquard dataset are also conducted. Figure 5 displays some examples of the predicted heatmaps and predicted grasps of GR-CNN, TF-Grasp, and HTC-Grasp. The results indicate that HTC-Grasp exhibits a higher grasping

quality compared to GR-CNN and TF-Grasp methods. Table 2 presents the statistical results of HTC-Grasp on the Jacquard dataset in comparison to several classic algorithms. HTC-Grasp outperformed the other algorithms with an accuracy of 95.8% and 92.4% for image and object-wise tests.

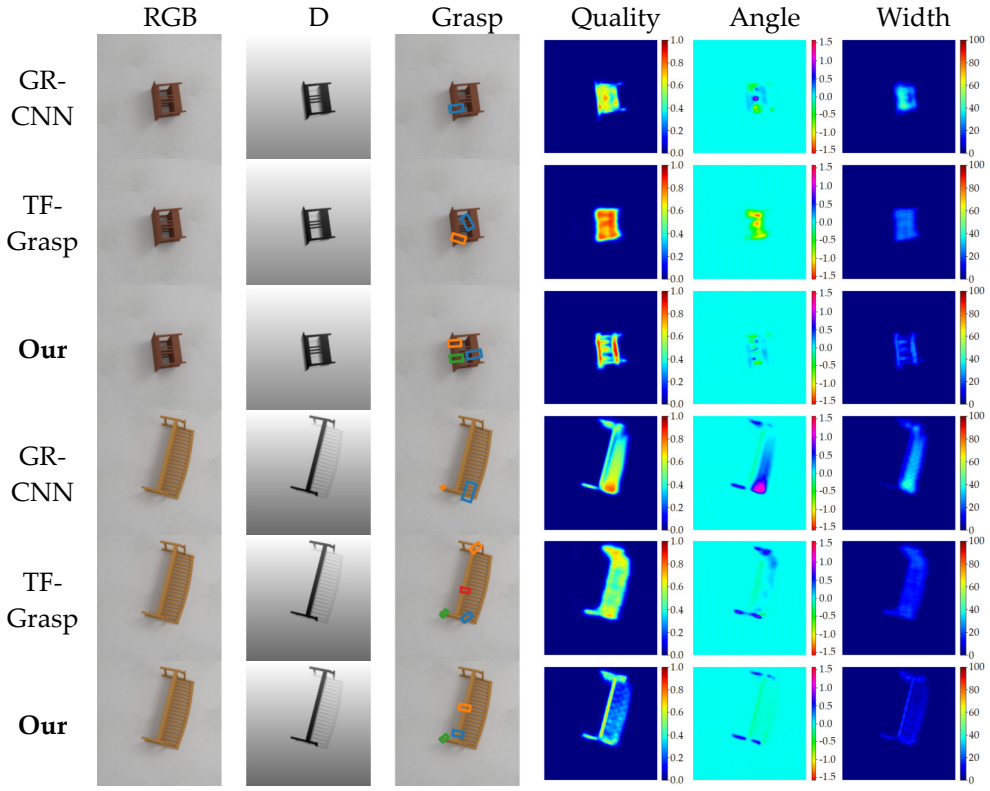

Figure 5. Comparison of predicted heatmaps on Jacquard Dataset. The first and second columns depict RGB and depth images, respectively. The third column displays the grasping rectangles and successful grasps are marked as rectangles. The final three columns depict heatmaps indicating the quality, angle, and width of the detected grasps. The quality heatmaps characterizes the degree of confidence that each pixel is a valid grasping location.

Table 2. The statistical results on Jacquard Dataset.

Researchers	Approaches	Data	Accuracy (%)	
			Image-Wise	Object-Wise
Morrision [14]	GG-CNN	D	84	-
Kumra [21]	GR-CNN	RGB-D	92.6	87.7
Wang [27]	TF-Grasp	RGB-D	94.6	-
Ours	HTC-Grasp	RGB-D	**95.8**	**92.4**

Qualitative comparison results for the Cornell and Jacquard datasets are demonstrated in Figures 4 and 5. It can be observed that:

(1) As shown in the first and third rows of Figures 4 and 5, the GR-CNN method which is solely based on CNNs has a low prediction quality in the central region of easily grasped objects. The background predictions by GRCNN are almost identical to actual grasping poses. This indicates that grasp pose detection is vulnerable to environmental interference. This is due to the absence of an attention mechanism in the GR-CNN network, leading to its poor performance.

(2) In comparison to the Transformer-based TF-Grasp model, the proposed HTC-Grasp provides more precise predictions of grasp quality and retains more detailed shape

information. This is achieved by incorporating an external attention mechanism in the encoder module, which enhances the network's capability to encode global context and differentiate semantics. Furthermore, a Residual Channel attention module is introduced into the decoder module, which allows the network to learn and determine the significance of each feature channel, thereby improving the utilization of valuable features and reducing the impact of redundant features.

Experimental results demonstrate that the HTC-Grasp approach can accurately identify suitable grasp locations and effectively differentiate graspable regions with a high level of confidence. As seen in the third and sixth rows of Figure 4, valid grasping pixels are highlighted with scores of approximating 1, while invalid pixels are marked with smaller values. Similarly in Figure 5, the protruding parts of the object that are easily graspable are precisely marked with a high score, and the model effectively captures both global information and fine-grained features such as the exact location and shape of the object.

To further evaluate HTC-Grasp's efficiency, experiments using a test set of images captured by ourselves without additional training are conducted. The results in Figure 6 indicate that HTC-Grasp can accurately identify grasp regions in an unseen real-world environment.

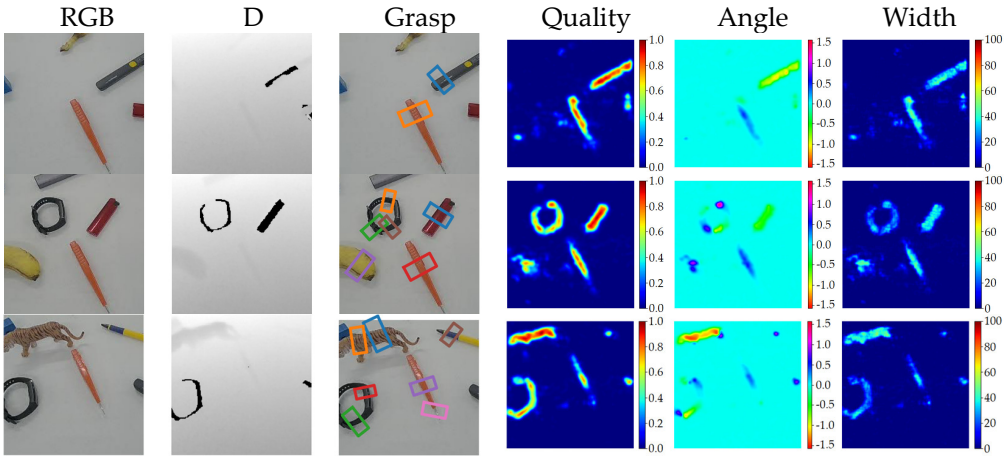

Figure 6. The test result of HTC-Grasp in the real-world multiple objects environment. The first and second columns depict RGB and depth images, respectively. The third column displays the grasping rectangles and successful grasps are marked as rectangles. The final three columns depict heatmaps indicating the quality, angle, and width of the detected grasps. The quality heatmaps characterizes the degree of confidence that each pixel is a valid grasping location.

4.3. Ablation Studies

To validate the impact of external attention and channel attention on the HTC-Grasp model, experiments on the same datasets are conducted. HTC-Grasp model is compared to versions without external attention and channel attention, respectively.

Table 3 shows the results of the ablation experiments. The results indicate that incorporating external attention in the encoder and channel attention in the decoder leads to improved performance. The external attention mechanism in the transformer effectively combines global features, leading to better results. Additionally, the Res-Channel attention blocks enhance the weight of effective feature maps, resulting in improved performance. The results demonstrate that both external attention and Res-Channel attention contribute to the accuracy of the final grasp box predictions.

Table 3. The comparison results on Jacquard Dataset.

	With External Attention	With Channel Attention	Accuracy (%)
Cornell Dataset	√		97.2
		√	97.6
	√	√	98.3
Jacquard Dataset	√		94.2
		√	94.7
	√	√	95.8

4.4. Grasping in Realistic Scenarios

4.4.1. Experimental Setup

In the grasping experiments, an Elite EC66 robot, a soft parallel manipulator and an Orbbec Femto-W camera are utilized as the experimental setup. As shown in Figure 7, the camera is positioned in a fixed location, and the image streams are captured by it. With the help of the Fin Ray effect-inspired soft gripper, the robot can grasp different shapes of targets adaptively without force control. For robot motion planning and control, open-source ROS is employed as the software platform. To verify the adaptability of the HTC-Grasp method to different shapes of grasping targets, more than 40 household objects are used in the experiment. As shown in Figure 8, these targets are to be grasped such as rectangular, cylindrical, circular and other objects of various shapes and sizes.

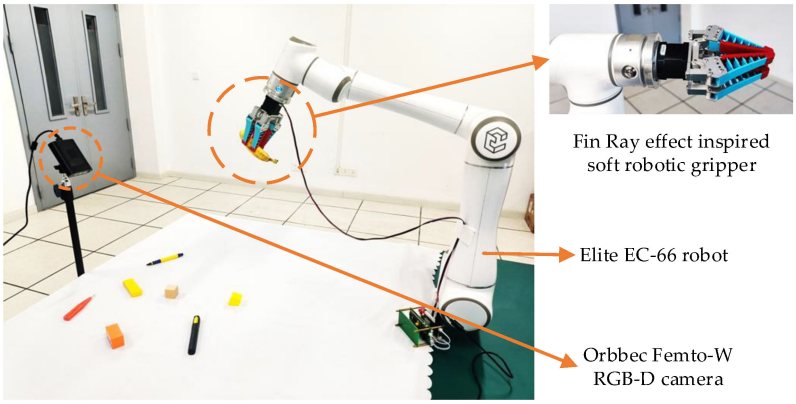

Figure 7. Realistic scenario experiment setup. The experimental equipment includes the Elite EC-66 robot, the Fin Ray effect-inspired soft parallel gripper and the Orbbec Femto-W RGB-D camera.

Figure 8. Household objects used in the experiment.

4.4.2. Experiment Results

The RGB-D camera captures video streams and fed them into the proposed model to obtain the best grasping pose. Subsequently, the robot's end actuator approaches the target according to the motion planning method, and the gripper is closed to grasp the target. The end actuator is then able to lift the object to another location.

Figure 9 illustrates the grasping process. A total of 180 grips were carried out to grasp household objects and the robot successfully grasped 168 times with an accuracy rate of 93.3%. The detailed results are presented in Table 4. The results demonstrate the effectiveness of the HTC-Grasp method in real-world robot grasping tasks. Some successful and unsuccessful grasp examples are shown in Appendices A and B.

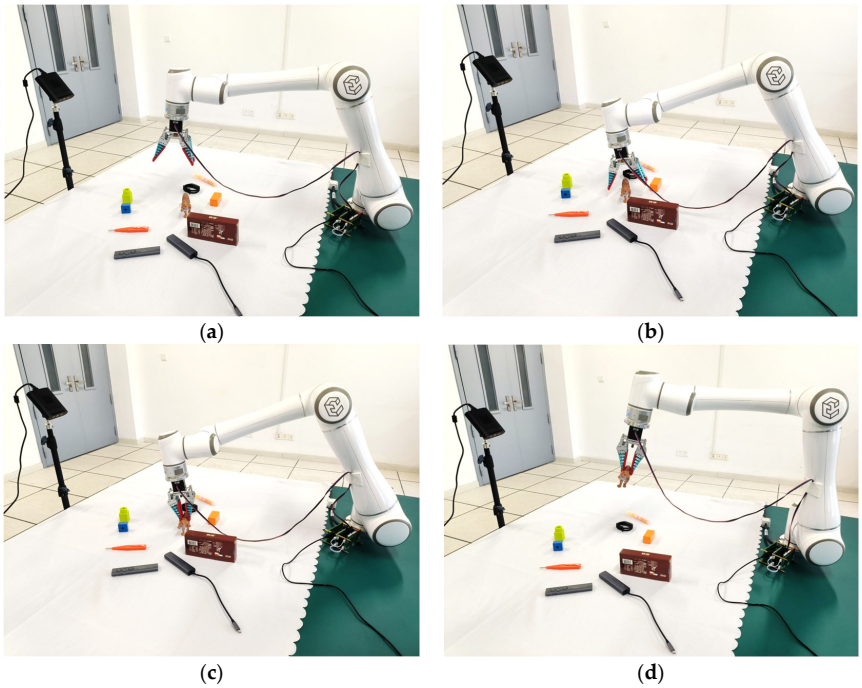

Figure 9. Example of the robotic grasp process. (**a**) shows the initial state of the robot. (**b**) illustrates the robot's gripper has moved to the target to be grasped. (**c**) shows the state of the object being grasped. (**d**) demonstrates the target being moved to another location.

Table 4. Grasp success rates in robotic grasping experiments.

Researchers	Physical Grasp	Success Rate
Lenz [15]	89/100	89.0%
Morrison [14]	110/120	92.0%
Chu [28]	89/100	89.0%
Wang [26]	152/165	92.1%
Ours	168/180	**93.3%**

According to the above argumentation experiment results, the HTC-Grasp method has excellent detection results in most cases. However, when faced with poor lighting conditions, transparency, reflections, etc., the accuracy of the proposed algorithm detection decreases.

5. Conclusions

This article proposes a novel hierarchical hybrid architecture that combines Transformer and convolutional neural network (CNN) for visual grasping in robotics. Specifically, the proposed architecture enhances the conventional CNN by incorporating an external

attention-based hierarchical Transformer, as the encoder, captures the global context, and generates more informative feature representations. Additionally, a channel-wise attention mechanism is introduced to adaptively adjust channel weights for efficient feature aggregation. The proposed architecture, HTC-Grasp, has been evaluated on two benchmark datasets, namely Cornell and Jacquard, and it was found that the proposed approach consistently outperformed existing state-of-the-art methods, leading to significant improvements in grasping accuracy.

Author Contributions: Conceptualization, Q.Z.; methodology, Q.Z. and J.Z.; software, Q.Z. and J.Z.; writing—original draft preparation, J.Z. and X.S.; writing—review and editing, Q.Z. and M.L.; visualization, X.S. All authors have read and agreed to the published version of the manuscript.

Funding: This research was funded by the National Natural Science Foundation of China (grant number 61903162) and Jiangsu Province's "Double Innovation Plan": Research and development of flexible cooperative robot technology for intelligent manufacturing.

Data Availability Statement: The data presented in this study are available on request from the corresponding author.

Conflicts of Interest: The authors declare no conflict of interest.

Appendix A Sample of Successful Grasps

The first and third columns shows the quality maps for each image. The quality heatmaps characterizes the degree of confidence that each pixel is a valid grasping location. Successful grasps are marked as blue rectangles in the second and the fourth columns.

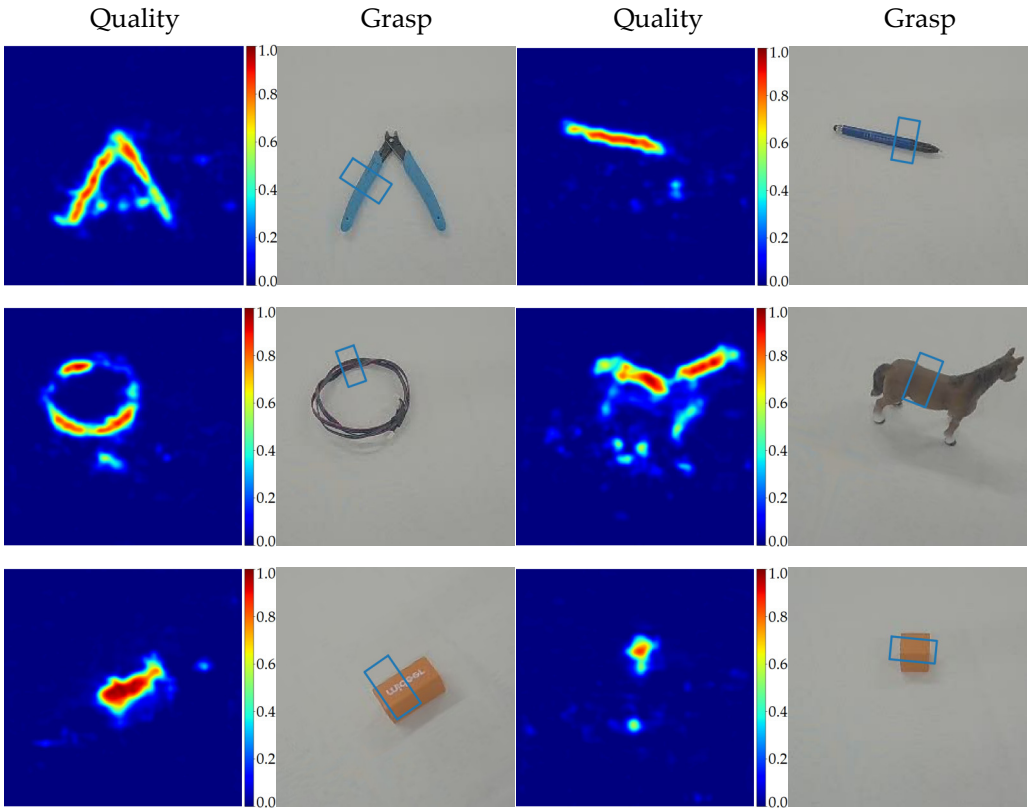

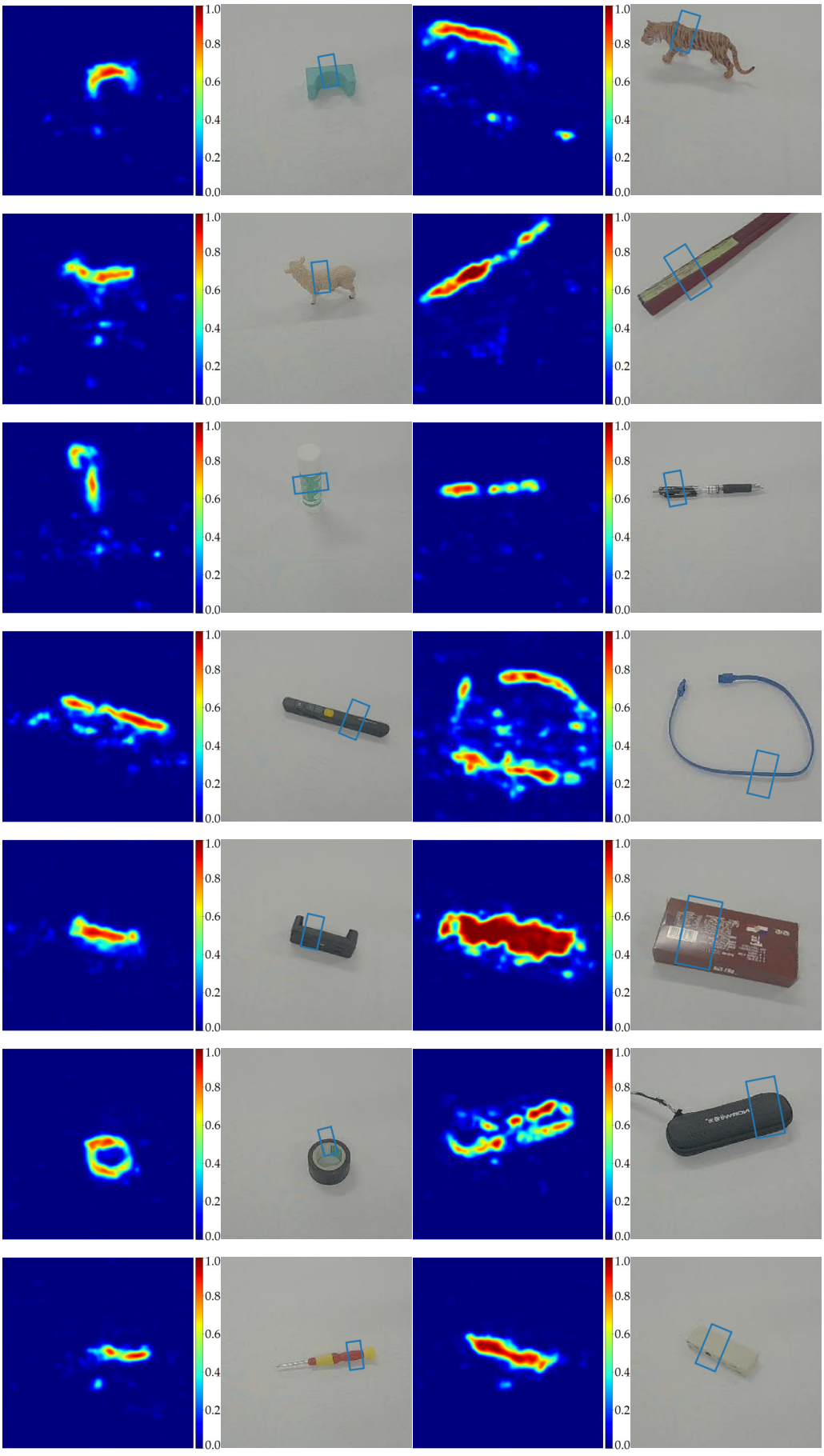
1.0
0.8
0.6
0.4
0.2
0.0

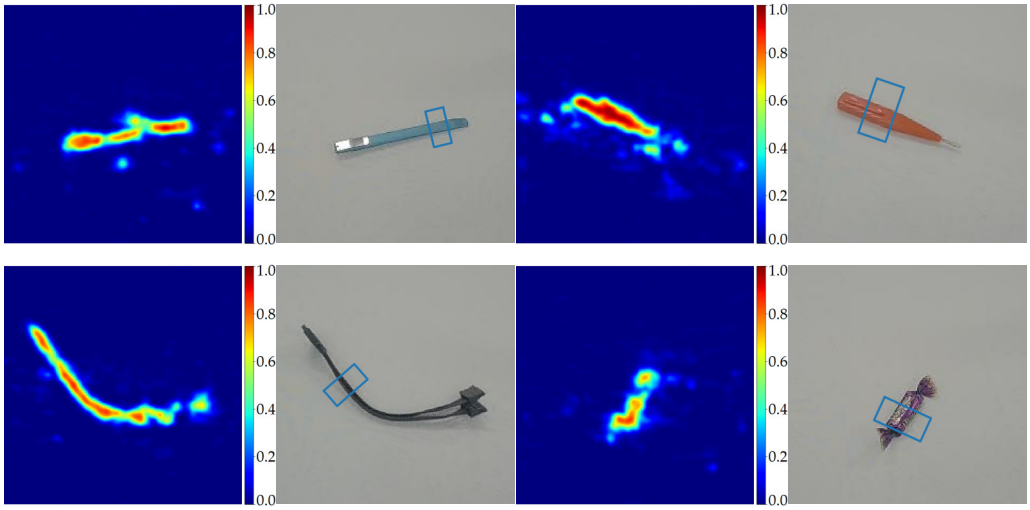

Appendix B Sample of Unsuccessful Grasps

The first and third columns shows the quality maps for each image. The quality heatmaps characterizes the degree of confidence that each pixel is a valid grasping location. Unsuccessful grasps are marked as blue rectangles in the second and the fourth columns.

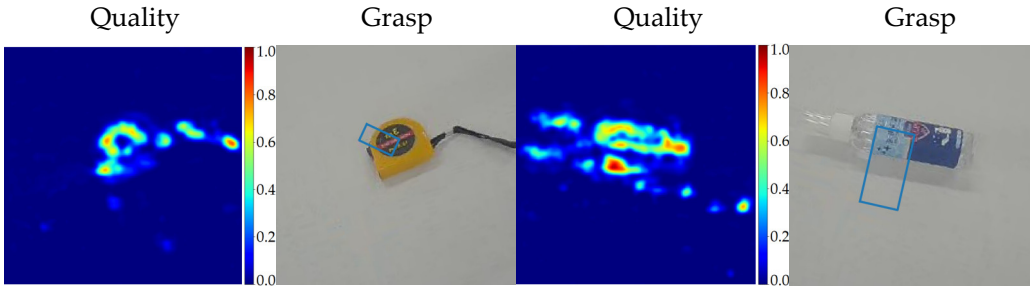

References

1. Tian, Y.; Chen, C.; Sagoe-Crentsil, K.; Zhang, J.; Duan, W. Intelligent Robotic Systems for Structural Health Monitoring: Applications and Future Trends. *Autom. Constr.* **2022**, *139*, 104273. [CrossRef]
2. Torres, R.; Ferreira, N. Robotic Manipulation in the Ceramic Industry. *Electronics* **2022**, *11*, 4180. [CrossRef]
3. Zhang, H.; Lan, X.; Bai, S.; Zhou, X.; Tian, Z.; Zheng, N. Roi-Based Robotic Grasp Detection for Object Overlapping Scenes. In Proceedings of the 2019 IEEE/RSJ International Conference on Intelligent Robots and Systems (IROS), Macau, China, 3–8 November 2019; pp. 4768–4775.
4. Du, G.; Wang, K.; Lian, S.; Zhao, K. Vision-Based Robotic Grasping from Object Localization, Object Pose Estimation to Grasp Estimation for Parallel Grippers: A Review. *Artif. Intell. Rev.* **2021**, *54*, 1677–1734. [CrossRef]
5. Sun, Y.; Falco, J.; Roa, M.A.; Calli, B. Research Challenges and Progress in Robotic Grasping and Manipulation Competitions. *IEEE Robot. Autom. Lett.* **2022**, *7*, 874–881. [CrossRef]
6. Pinto, L.; Gupta, A. Supersizing Self-Supervision: Learning to Grasp from 50k Tries and 700 Robot Hours. In Proceedings of the 2016 IEEE international Conference on Robotics and Automation (ICRA), Stockholm, Sweden, 16–21 May 2016; pp. 3406–3413.
7. Wang, Z.; Li, Z.; Wang, B.; Liu, H. Robot Grasp Detection Using Multimodal Deep Convolutional Neural Networks. *Adv. Mech. Eng.* **2016**, *8*, 1687814016668077. [CrossRef]
8. Asif, U.; Tang, J.; Harrer, S. GraspNet: An Efficient Convolutional Neural Network for Real-Time Grasp Detection for Low-Powered Devices. *Proc. IJCAI* **2018**, *7*, 4875–4882.
9. Karaoguz, H.; Jensfelt, P. Object Detection Approach for Robot Grasp Detection. In Proceedings of the 2019 International Conference on Robotics and Automation (ICRA), Montreal, QC, Canada, 20–24 May 2019; pp. 4953–4959.
10. Song, J.; Patel, M.; Ghaffari, M. Fusing Convolutional Neural Network and Geometric Constraint for Image-Based Indoor Localization. *IEEE Robot. Autom. Lett.* **2022**, *7*, 1674–1681. [CrossRef]
11. Dosovitskiy, A.; Beyer, L.; Kolesnikov, A.; Weissenborn, D.; Zhai, X.; Unterthiner, T.; Dehghani, M.; Minderer, M.; Heigold, G.; Gelly, S.; et al. An image is worth 16x16 words: Transformers for image recognition at scale. *arXiv* **2021**, arXiv:2010.11929.

12. Wang, W.; Xie, E.; Li, X.; Fan, D.-P.; Song, K.; Liang, D.; Lu, T.; Luo, P.; Shao, L. Pyramid Vision Transformer: A Versatile Backbone for Dense Prediction without Convolutions. In Proceedings of the 2021 IEEE/CVF International Conference on Computer Vision (ICCV), Montreal, QC, Canada, 10–17 October 2021; pp. 548–558.
13. Jiang, Y.; Moseson, S.; Saxena, A. Efficient Grasping from RGBD Images: Learning Using a New Rectangle Representation. In Proceedings of the 2011 IEEE International Conference on Robotics and Automation, Shanghai, China, 9–13 May 2011; pp. 3304–3311.
14. Morrison, D.; Corke, P.; Leitner, J. Learning Robust, Real-Time, Reactive Robotic Grasping. *Int. J. Robot. Res.* **2020**, *39*, 183–201. [CrossRef]
15. Lenz, I.; Lee, H.; Saxena, A. Deep Learning for Detecting Robotic Grasps. *Int. J. Robot. Res.* **2015**, *34*, 705–724. [CrossRef]
16. Zhou, X.; Lan, X.; Zhang, H.; Tian, Z.; Zhang, Y.; Zheng, N. Fully Convolutional Grasp Detection Network with Oriented Anchor Box. In Proceedings of the 2018 IEEE/RSJ International Conference on Intelligent Robots and Systems (IROS), Madrid, Spain, 1–5 October 2018; pp. 7223–7230.
17. Laili, Y.; Chen, Z.; Ren, L.; Wang, X.; Deen, M.J. Custom Grasping: A Region-Based Robotic Grasping Detection Method in Industrial Cyber-Physical Systems. *IEEE Trans. Autom. Sci. Eng.* **2023**, *20*, 88–100. [CrossRef]
18. Redmon, J.; Angelova, A. Real-Time Grasp Detection Using Convolutional Neural Networks. In Proceedings of the 2015 IEEE International Conference on Robotics and Automation (ICRA), Seattle, WA, USA, 26–30 May 2015; pp. 1316–1322.
19. Kumra, S.; Kanan, C. Robotic Grasp Detection Using Deep Convolutional Neural Networks. In Proceedings of the 2017 IEEE/RSJ International Conference on Intelligent Robots and Systems (IROS), Vancouver, BC, Canada, 24–28 September 2017; pp. 769–776.
20. Kumra, S.; Joshi, S.; Sahin, F. Antipodal Robotic Grasping Using Generative Residual Convolutional Neural Network. In Proceedings of the 2020 IEEE/RSJ International Conference on Intelligent Robots and Systems (IROS), Las Vegas, NV, USA, 25–29 October 2020; pp. 9626–9633.
21. Mahler, J.; Liang, J.; Niyaz, S.; Laskey, M.; Doan, R.; Liu, X.; Aparicio, J.; Goldberg, K. Dex-Net 2.0: Deep Learning to Plan Robust Grasps with Synthetic Point Clouds and Analytic Grasp Metrics. In Proceedings of the Robotics: Science and Systems XIII, Robotics: Science and Systems Foundation, Cambridge, MA, USA, 12–16 July 2017.
22. Yu, S.; Zhai, D.-H.; Xia, Y.; Wu, H.; Liao, J. SE-ResUNet: A Novel Robotic Grasp Detection Method. *IEEE Robot. Autom. Lett.* **2022**, *7*, 5238–5245. [CrossRef]
23. Wu, Y.; Zhang, F.; Fu, Y. Real-Time Robotic Multigrasp Detection Using Anchor-Free Fully Convolutional Grasp Detector. *IEEE Trans. Ind. Electron.* **2021**, *69*, 13171–13181. [CrossRef]
24. Liu, Z.; Lin, Y.; Cao, Y.; Hu, H.; Wei, Y.; Zhang, Z.; Lin, S.; Guo, B. Swin Transformer: Hierarchical Vision Transformer Using Shifted Windows. In Proceedings of the IEEE/CVF International Conference on Computer Vision, Virtual, 11–17 October 2021; pp. 10012–10022.
25. Xie, E.; Wang, W.; Yu, Z.; Anandkumar, A.; Alvarez, J.M.; Luo, P. SegFormer: Simple and Efficient Design for Semantic Segmentation with Transformers. *Adv. Neural Inf. Process. Syst.* **2021**, *34*, 12077–12090.
26. Wang, S.; Zhou, Z.; Kan, Z. When Transformer Meets Robotic Grasping: Exploits Context for Efficient Grasp Detection. *IEEE Robot. Autom. Lett.* **2022**, *7*, 8170–8177. [CrossRef]
27. Guo, M.-H.; Liu, Z.-N.; Mu, T.-J.; Hu, S.-M. Beyond Self-Attention: External Attention Using Two Linear Layers for Visual Tasks. *IEEE Trans. Pattern Anal. Mach. Intell.* **2022**. *early access*. [CrossRef] [PubMed]
28. Chu, F.-J.; Xu, R.; Vela, P.A. Real-World Multiobject, Multigrasp Detection. *IEEE Robot. Autom. Lett.* **2018**, *3*, 3355–3362. [CrossRef]